ELSEVIER

Coordination Chemistry Reviews
174 (1998) 241–253

COORDINATION CHEMISTRY REVIEWS

# The use of $C_3$-symmetric tripodal ligands in crystal engineering

Brian S. Hammes [b], Dorisa Ramos-Maldonado [b], Glenn P.A. Yap [c], Arnold L. Rheingold [c], Victor G. Young, Jr.[d], A.S. Borovik [a,*]

[a] *Department of Chemistry, University of Kansas, Lawrence, KS 66045, USA*
[b] *Department of Chemistry, Kansas State University, Manhattan, KS 66506, USA*
[c] *Department of Chemistry, University of Delaware, Newark, DE 19716, USA*
[d] *Department of Chemistry, University of Minnesota, Minneapolis, MN 55455, USA*

Received 20 August 1997; accepted 14 January 1998

**Contents**



**Abstract**

The use of chiral tripodal ligands in the assembly of non-centrosymmetric crystal lattice is illustrated with the triamide ligand tris[*N*-(*S*)-(−)-(α)-methylbenzylcarbamoylmethyl]amine ($H_3I^{S\text{-}mbz}$). In the crystal phase, this tripodal ligand assembles into $C_3$-symmetric chiral columns that are stabilized by hydrogen bonds and aryl–aryl interactions. Intercolumnar assembly is driven by the clustering of edge-to-face aryl and methyl-to-aryl interactions. Thrice deprotonation of $H_3I^{S\text{-}mbz}$ and binding of an Ni(II)–F moiety also produces a non-

* Corresponding author. Fax: +1 785 864 5398; e-mail: aborovik@caco3.chem.ukans.edu


*PII* S0010-8545(98)00051-4

centrosymmetric lattice which is noteworthy for its six-fold symmetric open framework structure and the alignment of all the molecular Ni–F bonds in the lattice along the crystallographic $c$-axis. Crystal data: $H_3\mathbf{1}^{S\text{-mbz}}$ crystallizes in the rhombohedral system, space group $R3$ with cell dimensions $a=b=22.352(5)$ Å, $c=4.882(1)$ Å, $\alpha=\beta=90°$, $\gamma=120°$, and $Z=3$; $[NEt_4]_2[Ni\mathbf{1}^{S\text{-mbz}}(F)]$ crystallizes in the hexagonal system, space group $P6_3$ with cell dimensions $a=b=12.0780(1)$ Å, $c=18.1231(1)$ Å, $\alpha=\beta=90°$, $\gamma=120°$, and $Z=2$. 

## 1. Introduction

The development of metal complexes that assemble into predictable supramolecular structures in the crystal phase is of great interest because of their potential in designing new materials that have desirable optical or magnetic properties [1–3]. However, several factors can influence crystal lattice assembly, including counterion(s), solvent, and the geometries of the ligands bonded to the metal ion(s) [4]. These factors have limited our ability to accurately predict structure, especially in cases where chiral lattices are required. We have been designing organic chelating ligands that upon metal binding can direct the assembly of chiral supramolecular arrays. Our previous systems have used helical motifs having $C_2$ molecular symmetry that assemble into chiral arrays where non-covalent interactions are the dominant intermolecular forces [5,6]. In this report we describe the molecular and crystal structures of the homochiral $C_3$-symmetric tripodal ligand tris[*N*-(*S*)-(−)-(α)-methylbenzylcarbamoylmethyl]amine ($H_3\mathbf{1}^{S\text{-mbz}}$) [7–10].

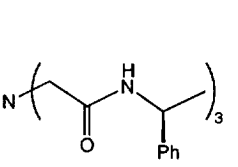


$H_3\mathbf{1}^{S\text{-mbz}}$

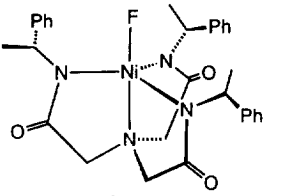


$[Ni\mathbf{1}^{S\text{-mbz}}(F)]^{2-}$

The self-complementary character of this ligand controls its assembly into aggregrates via intermolecular hydrogen bonds and edge-to-face aryl interactions. (For the use of self-complementary molecules in assembly processes, see ref. [11].) This chiral ligand maintains its three-fold symmetry upon deprotonation and binding a small metal-containing fragment, as is illustrated by the isolation and single crystal structural analysis of $[NEt_4]_2[Ni\mathbf{1}^{S\text{-mbz}}(F)]$. The lattice structure of this compound is noteworthy for its six-fold symmetry and the alignment of all the molecular Ni–F bonds in the lattice along the crystallographic $c$-axis.

## 2. Experimental

All reagents and solvents were purchased from commercial sources and used as received, unless noted otherwise. Pyridine (Aldrich) was distilled over KOH (5 g

KOH per 50 ml pyridine) under $N_2$. Flash chromatography was carried out on 230–400 mesh chromatographic silica gel (Fisher). Metal complex preparation was conducted under an argon atmosphere in a Vacuum Atmospheres model #MO-20-SSG drybox. Elemental analysis of all compounds was performed by Desert Analytics, Inc., Tucson, AZ. All samples were dried in vacuo prior to analysis.

### 2.1. *Tris[N-(S)-(−)-(α)-methylbenzylcarbamoylmethyl]amine* ($H_3\mathbf{1}^{S\text{-}mbz}$)

Nitrilotriacetic acid (2.00 g, 10.5 mmol) was added to 40 ml of pyridine. The slurry was stirred vigorously while (*S*)-(−)-(α)-methylbenzylamine (3.80 g, 31.4 mmol, 99% ee/GLC) was added. The solution was warmed to 50 °C and triphenylphosphite (9.74 g, 31.4 mmol) was added. Heating continued until the temperature reached 105 °C. After 1 h at this temperature the reaction became a colorless homogeneous mixture which was allowed to stir for an additional 4 h. The volatiles were removed by vacuum distillation and the resulting yellow oil was dissolved in $CHCl_3$ and washed three times with 100 ml of $H_2O$, eight times with 100 ml of aqueous saturated $NaHCO_3$, twice with 100 ml of $H_2O$, once with brine and dried over $MgSO_4$. Purification of the ligand was accomplished by flash chromatography over silica gel with 95:5 $CHCl_3$:$CH_3OH$ as the eluent to yield 3.16 g (61%) of $H_3\mathbf{1}^{S\text{-}mbz}$. M.p. 149–152 °C (uncorrected); $^1$H NMR ($(CD_3)_2SO$): $\delta$ 8.63 (d, 1 H, $J=7$ Hz, –C(O)N*H*); 7.27 (m, 5 H, –Ar*H*); 4.96 (dq, 1 H, $J=7$ Hz, –C*H*–); 3.34 (d, 1 H, $J=16$ Hz, –C*H*H–); 3.29 (d, 1 H, $J=16$ Hz, –CH*H*–); 1.34 (d, 3 H, $J=7$ Hz, –C$H_3$); $^{13}$C NMR ($CDCl_3$): $\delta$ 169.77, 143.49, 128.82, 127.50, 126.36, 61.13, 49.23, 22.35; FTIR (Nujol, $cm^{-1}$), $\nu$(NH) 3475 (s); $\nu$(CO) 1658 (vs); $[\alpha]^{25}=-45\pm0.2$ ($c=1.4$, DMF); $MH^+$ *m/e*: 501 (FAB); Anal. Calc. (Found) for $H_3\mathbf{1}^{S\text{-}mbz}$, $C_{30}H_{36}N_4O_3$: C, 71.96 (71.44); H, 7.26 (7.39); N, 11.18 (11.14).

### 2.2. *Tetraethylammonium fluoro{tris[N-(S)-(−)-(α)-methylbenzylcarbamoylmethyl] aminato}nickelate(II)* $[NEt_4]_2[Ni\mathbf{1}^{S\text{-}mbz}(F)]$

A DMF solution of $H_3\mathbf{1}^{S\text{-}mbz}$ (0.30 g, 0.96 mmol) was treated with potassium hydride (0.12 g, 2.9 mmol). After $H_2$ evolution had ceased, 0.17 g (0.96 mmol) $Ni(OAc)_2$ was added slowly. After 1 h the mixture was filtered and the precipitate (KOAc) was discarded. The solvent was removed under vacuum and the resulting oil was washed with THF and diethyl ether to give 0.37 g of an orange solid. Without further purification 0.19 g (0.32 mmol) of the orange solid was redissolved in 5 ml of DMF and $Et_4NCl$ (0.053 g, 0.32 mmol) was added. The solution was stirred for 1 h, filtered, and the precipitate (KCl) was discarded. The filtrate was concentrated to dryness under vacuum affording an orange solid which was dissolved in $CH_3CN$ and treated with solid $Et_4NF$ (0.050 g, 0.32 mmol). The resulting yellow solution was stirred for an additional 30 min, filtered, and the solution was concentrated under reduced pressure and crystallized by slow diffusion of diethyl ether into this solution to give 0.13 g (47%) of $[NEt_4]_2[Ni\mathbf{1}^{S\text{-}mbz}(F)]$. FTIR (Nujol, $cm^{-1}$) $\nu$(CO) 1586 (s); 1568 (sh); 1559 (s); $\mu_{eff}=3.19\,\mu_B$ (solid, 298 K); $\lambda_{max}$ ($CH_3CN$, $M^{-1}\,cm^{-1}$) = 326 (720), 429 (105), 510 (sh), 678 (28), 782 (21);

$\lambda_{max}$ ($CH_3CN$, $\Delta\epsilon$, $M^{-1}\,cm^{-1}$)=439 (−0.284), 502 (−0.310), 672 (−0.343); Anal. Calc. (Found) for {$(Et_4N)_2$[Ni$\mathbf{1}^{S\text{-mbz}}$(F)]}, $C_{46}H_{73}FN_6NiO_3$: C, 66.09 (65.97); H, 8.82 (8.80); N, 10.05 (9.85).

### 2.3. Physical methods

$^1H$ and $^{13}C$ NMR spectra were collected on a Varian UNITY Plus-400 NMR spectrometer equipped with a Sun workstation. Chemical shifts are reported in parts per million relative to an internal standard of TMS. FTIR spectra were recorded on a Matteson Sirius 100 FTIR spectrometer (with 4326 upgrade) interfaced to a Tangent 486 MHz computer and are reported in wavenumbers. Electronic spectra were recorded using a SLM-Aminco 3000 diode array spectrophotometer. Fast atom bombardment mass spectra (FAB-MS) were recorded on a Hewlett-Packard 5989A spectrometer. Room temperature magnetic susceptibility measurements of the solid state samples were determined using a magnetic susceptibility balance MSB-1 manufactured by Johnson Matthey and calibrated with mercury(II) tetrathiocyanatocobaltate(II) ($\chi_g = 16.44 \times 10^{-6} \pm 0.08\ cm^3\ g^{-1}$) [12].

### 2.4. Crystallographic structural determination

Crystal data collection and refinement parameters for $H_3\mathbf{1}^{S\text{-mbz}}$ and [$NEt_4$]$_2$[Ni$\mathbf{1}^{S\text{-mbz}}$(F)] are given in Table 1. The systematic absences in the diffraction data are consistent with the space groups $P6_3$ and $R3$ for [$NEt_4$]$_2$[Ni$\mathbf{1}^{S\text{-mbz}}$(F)] and $H_3\mathbf{1}^{S\text{-mbz}}$. The structures were solved using direct methods, completed by subsequent difference Fourier synthesis and refined by full-matrix least-squares procedures. For [$NEt_4$]$_2$[Ni$\mathbf{1}^{S\text{-mbz}}$(F)], only the nitrogen atoms of the tetraethylammonium cations were well-behaved; the ethyl groups were severely disordered. Therefore, only the nitrogen atoms were included in the atom list and the data were processed with PLATON/SQUEEZE [13]. The cation volume was determined to be 990.7 Å$^3$ out of a cell volume of 2289.6 Å$^3$. The data were corrected for 180 electrons worth of diffuse scattering. All non-hydrogen atoms were refined with anisotropic displacement coefficients and hydrogen atoms were treated as idealized contributions. All software sources of the scattering factors are contained in the SHELXTL (5.3) program library (G. Sheldrick, Siemens XRD, Madison, WI).

## 3. Results and discussion

### 3.1. Solid state structure of $H_3\mathbf{1}^{S\text{-mbz}}$

The tripodal character of $H_3\mathbf{1}^{S\text{-mbz}}$ arises from the three carbamoylmethyl arms surrounding a central amine nitrogen. The chirality in this compound is located at the amide ends of each tripodal arm where optically pure (*S*)-(−)-(α)-methylbenzyl groups are appended from the amide nitrogens. We had anticipated that the placement of these chiral groups next to the amide moieties, which have the potential to

Table 1
Summary of crystallographic data and parameters for $H_3\mathbf{1}^{S\text{-mbz}}$ and $[NEt_4]_2[Ni\mathbf{1}^{S\text{-mbz}}(F)]$

| Complex | $H_3\mathbf{1}^{S\text{-mbz}}$ | $(NEt_4)_2[Ni\mathbf{1}^{S\text{-mbz}}(F)]$ |
|---|---|---|
| Molecular formula | $C_{30}H_{36}N_4O_3$ | $C_{46}H_{73}FN_6NiO_3$ |
| *FW* | 500.63 | 835.81 |
| Temperature (K) | 298(2) | 173(2) |
| Crystal system | rhombohedral | hexagonal |
| Space group | *R*3 | $P6_3$ |
| Cell constants | | |
| *a* (Å) | 22.352(5) | 12.0780(1) |
| *b* (Å) | 22.352(5) | 12.0780(1) |
| *c* (Å) | 4.882(1) | 18.1231(1) |
| $\alpha$ (deg) | 90 | 90 |
| $\beta$ (deg) | 90 | 90 |
| $\gamma$ (deg) | 120 | 120 |
| *Z* | 3 | 2 |
| *V* (Å$^3$) | 2112(1) | 2289.57(3) |
| Absolute coefficient, $\mu_{calc}$ ($cm^{-1}$) | 0.77 | 4.73 |
| $\delta_{calc}$ (g/cm$^3$) | 1.181 | 1.212 |
| *F*(000) | 804 | 904 |
| Crystal dimensions (mm$^3$) | 0.40 × 0.20 × 0.20 | 0.42 × 0.35 × 0.32 |
| Radiation | Mo Kα ($\lambda$=0.71073 Å) | Mo Kα ($\lambda$=0.71073 Å) |
| *h*, *k*, *l* Ranges collected | −1→23, −24→1, −1→5 | −11→0, 0→14, −21→17 |
| $\theta$ Range (deg) | 3.16 to 22.44 | 1.95 to 25.05 |
| No. of reflections collected | 941 | 2490 |
| No. of independent reflections | 825 | 2490 |
| No. of parameters | 113 | 125 |
| Data/parameter ratio | 7.30 | 19.92 |
| Refinement method | full-matrix least-squares on $F^2$ | full-matrix least-squares on $F^2$ |
| $R^a$ | 0.0402 | 0.0707 |
| $wR_2^b$ | 0.1000 | 0.1789 |
| GOF[c] | 1.141 | 0.987 |
| Largest difference peak and hole (e/Å$^3$) | 0.093 and −0.128 | 0.680 and −0.290 |

[a] $R=[\Sigma|\Delta F|/\Sigma|F_o|]$.
[b] $R_w=[\Sigma w(\Delta F)^2/\Sigma wF_o^2]$.
[c] Goodness of fit on $F^2$.

hydrogen bond, would influence the assembly of the crystal lattice. Hence, crystallization of $H_3\mathbf{1}^{S\text{-mbz}}$ resulted in colorless sheet-like crystals belonging to the non-centrosymmetric space group *R*3. A representation of the molecular structure of $H_3\mathbf{1}^{S\text{-mbz}}$ is located in Fig. 1. Each $H_3\mathbf{1}^{S\text{-mbz}}$ molecule sits on a crystallographic three-fold axis where the three tripodal arms are symmetrically positioned around the central amine nitrogen. The three amide moieties in each molecule of $H_3\mathbf{1}^{S\text{-mbz}}$ are oriented such that the carbonyl groups are on one molecular face with the NH bonds positioned on the opposite face. The radially symmetric orientation of amide groups produces supramolecular $C_3$-symmetric columns that are aligned parallel

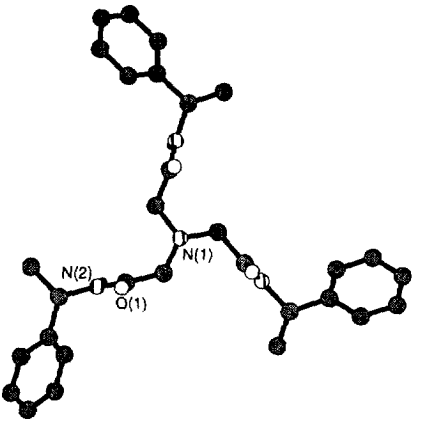


Fig. 1. View of the molecular structure of $H_3\mathbf{1}^{S\text{-mbz}}$ illustrating the $C_3$ rotational symmetry of the molecule.

with the crystallographic *c*-axis. Each column is stabilized by a network of hydrogen bonds where individual molecules in a column participate in three intermolecular hydrogen bonds with both of its nearest neighbors (Fig. 2). The positioning of $H_3\mathbf{1}^{S\text{-mbz}}$ molecules within a column is ideal for the formation of intermolecular hydrogen bonds, as is indicated by the short N···O distance of 2.846 Å and the nearly linear N–H–O angle of 179.4°. In addition, an individual molecule is involved in three aryl–aryl stacking interactions with each adjacent molecule within a column. The aryl rings of the methylbenzyl groups of the tripodal arms have π–π stacking interactions at a distance of 4.887 Å (centroid-to-centroid) which causes the stacked rings to have identical orientations (Fig. 2).

Intercolumnar stabilization is dominated by edge-to-face aryl and methyl-to-aryl interactions. Every column is surrounded by six other columns, three of which are

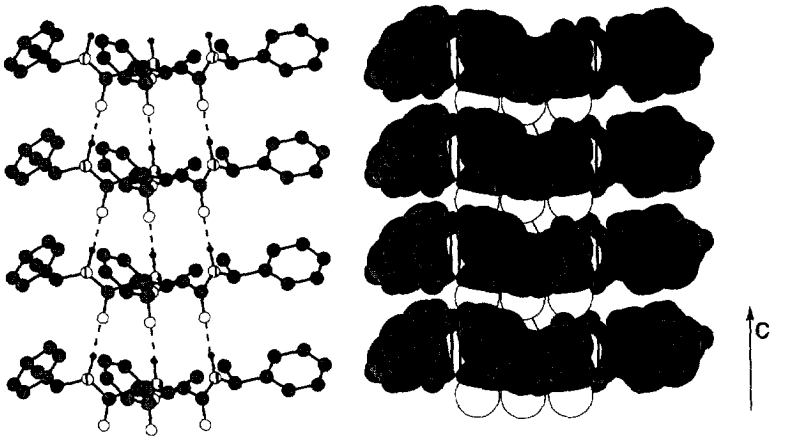


Fig. 2. A portion of the crystal lattice for $H_3\mathbf{1}^{S\text{-mbz}}$ (view of the *b*, *c* plane) showing the column motif.

in-register and three columns are out-of-register, offset by one-third of a unit cell as required by the *R*3 crystal symmetry (Fig. 4). This ordering results in each tripodal arm of an individual molecule within a column having two edge-to-face aryl interactions with molecules of adjacent columns where the aryl centroid–centroid distances are 5.397 and 6.089 Å [14–22]. In addition, two intercolumn methyl-to-aryl interactions per tripodal arm are observed at distances of 4.448 and 5.145 Å (methyl carbon to aryl centroid). These intercolumnar interactions result in an interlocking pattern of molecules in the *a*, *b* plane as is illustrated in Fig. 3. Note that all the molecules in the *a*, *b* plane have their amide groups aligned in the same direction, in keeping with the chiral character of the crystal.

The columnar motif found in the crystal lattice of $H_3\mathbf{1}^{S\text{-mbz}}$ resembles that found by Hamilton and coworkers for the 6-picoline derivative of *cis,cis*-cyclohexane-1,3,5-tricarboxamide [23]. In this compound, which also crystallized in

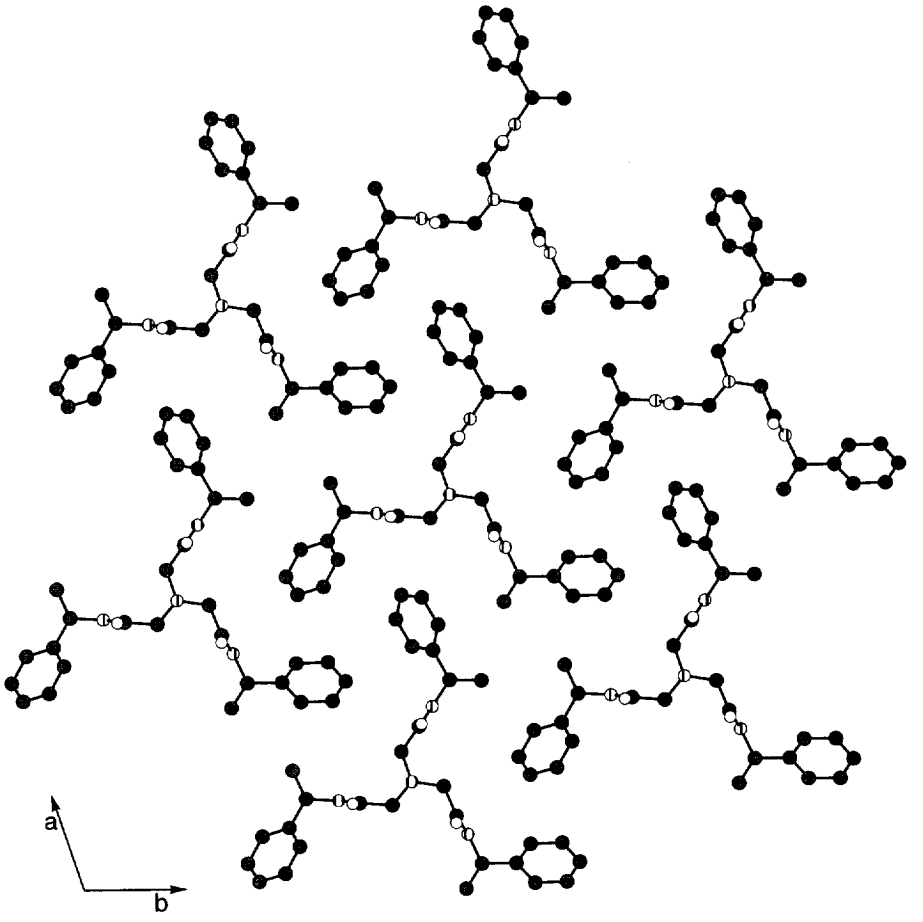


Fig. 3. A portion of the crystal lattice for $H_3\mathbf{1}^{S\text{-mbz}}$ (view of the *a*, *b* plane).

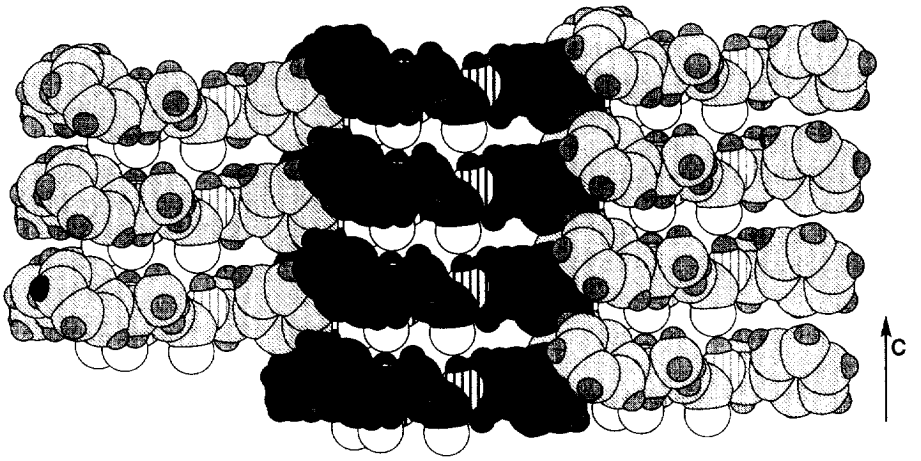


Fig. 4. The crystal structure of $H_3\mathbf{1}^{S\text{-mbz}}$ showing the intercolumn interactions within the crystal lattice (view of the *b*, *c* plane).

a trigonal space group (*R*3*c*), the cyclohexyl group was used to create disc-shaped molecules containing carboxamide groups at the periphery. A similar intracolumn hydrogen bond network observed in $H_3\mathbf{1}^{S\text{-mbz}}$ is present in Hamilton's system which has an N···O distance of 2.946 Å and an N–H–O angle of 162°. However, the intercolumn aryl interactions appear to be more extensive in $H_3\mathbf{1}^{S\text{-mbz}}$ than in Hamilton's systems: this undoubtedly results from the increased order obtained by positioning chiral groups at the periphery of the tripodal arms in $H_3\mathbf{1}^{S\text{-mbz}}$.

### 3.2. Solid state structure of $[NEt_4]_2[Ni\mathbf{1}^{S\text{-mbz}}(F)]$

We have previously shown that $[\mathbf{1}^{S\text{-mbz}}]^{3-}$, formed by deprotonating each amide group in $H_3\mathbf{1}^{S\text{-mbz}}$, binds metal ions with tetradentate coordination [7–10]. The methylbenzyl groups appended to each amide nitrogen act as scaffolding for the generation of chiral cavities whose structures are affected by the binding of external ligands. We were interested in the effects of placing a fluoride ion inside a chiral cavity because of its relatively small radius and high electronegativity. Specifically, we wanted to investigate: (i) if binding fluoride ions would order the methylbenzyl groups to form $C_3$-symmetric chiral complexes; and (ii) whether a non-centrosymmetic metal-containing lattice would form that had unusual structural features.

$[NEt_4]_2[Ni\mathbf{1}^{S\text{-mbz}}(F)]$ crystallized as yellow block crystals in the non-centrosymmetic space group $P6_3$. The molecular structure of $[Ni\mathbf{1}^{S\text{-mbz}}(F)]^{2-}$ is shown in Fig. 5 and reveals that the complex has a trigonal bipyramidal coordination geometry around the Ni(II) ion. The three amidate nitrogens of $[\mathbf{1}^{S\text{-mbz}}]^{3-}$ are arranged in the trigonal plane with a $Ni–N_{amid}$ distance of 2.073(4) Å and an interplanar $N_{amid}–Ni(1)–N_{amid}$ angle of 116.54(7)°. The $Ni–N_{amid}$ distance found in $[Ni\mathbf{1}^{S\text{-mbz}}(F)]^{2-}$ is similar to those reported for related Ni(II)–amidate complexes

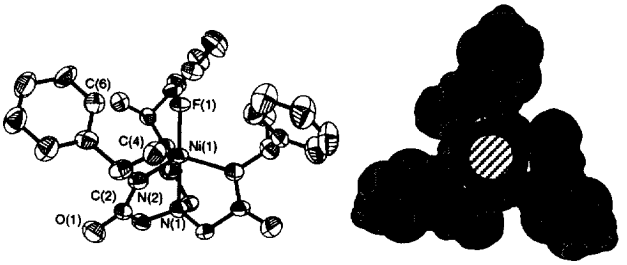


Fig. 5. Thermal ellipsoid diagram of $[Ni1^{S\text{-}mbz}(F)]^{2-}$ and a space-filling representation of the complex. The ellipsoids are drawn at the 40% probability level and hydrogens are omitted for clarity. Selected bond distances (Å) and angles (°): Ni(1)–F(1)=1.950(6); Ni(1)–N(1)=2.104(10); Ni(1)–N(2)=2.073(4); C(6)–F(1)=3.165; N(1)–Ni(1)–F(1)=180.000(2); N(2)–Ni(1)–F(1)=100.86(11); N(2)–Ni(1)–N(1)=79.15(11); N(2)–Ni(1)–N(2)#2=116.54.

[24–26]. The fluoro ligand is apically bonded to the Ni(II) center [Ni–F distance of 1.950(6) Å], a distance slightly shorter than those reported for other monomeric Ni–F complexes which have an average value of 2.036 Å [27–29]. The bound fluoro ligand is positioned *trans* to nitrogen N(1) of $[\mathbf{1}^{S\text{-}mbz}]^{3-}$ with the Ni ion located 0.39 Å above the trigonal plane toward the coordinated fluoride ion.

$[Ni1^{S\text{-}mbz}(F)]^{2-}$ possesses $C_3$-symmetry where the axis coincides with the F–Ni–N(1) vector. The appended methylbenzyl groups are thus symmetrically disposed around the bonded fluoro ligand to form a chiral cavity of alternating aryl and methyl moieties. Each aryl ring in $[Ni1^{S\text{-}mbz}(F)]^{2-}$ is positioned such that the C(6) hydrogen is directed toward the coordinated fluoro ligand with a C(6)H···F distance of 2.251 Å. The methyl moieties of the appended groups also interact with the fluoro ligand where the C(4)H···F distance is 2.444 Å. Both of these distances are within the range reported for other systems which have CH···F interactions [30]. (For a discussion on the possible use of CH···F interactions in crystal engineering, see refs. [31,32].) We suggest that these CH···F interactions are of sufficient strength to direct, in part, the orientation of the methylbenzyl groups in the chiral cavity (vide infra). Support for this suggestion comes from comparing the cavity structure in $[Ni1^{S\text{-}mbz}(F)]^{2-}$ to those found in the Zn(II) and Fe–NO complexes of $[\mathbf{1}^{S\text{-}mbz}]^{3-}$ [7]. In these latter systems, the major intracavity interactions are Ph···Me that arise from interactions between adjacent arms. This type of interaction produces a cavity structure that is significantly different from that observed in $[Ni1^{S\text{-}mbz}(F)]^{2-}$, where intracavity Ph···Me interactions are absent.

Figs. 6–8 show the crystal lattice packing for $[NEt_4]_2[Ni1^{S\text{-}mbz}(F)]$. For this salt, the packing pattern in the *a*, *b* plane is similar to that found for $H_3\mathbf{1}^{S\text{-}mbz}$: each anion is surrounded by six neighboring anions within the *a*, *b* plane where intermolecular edge-to-face aryl interactions are the dominant packing forces. The aryl groups of each tripodal arm are involved in two edge-to-face aryl interactions at a centroid-to-centroid distance of 5.622 Å. Layers of $[Ni1^{S\text{-}mbz}(F)]^{2-}$ anions are thus observed in the *a*, *b* plane with each anionic layer being separated by a layer of tetraethylammoniun cations [Fig. 6(b)]. Unfortunately, the ethyl groups of each cation are

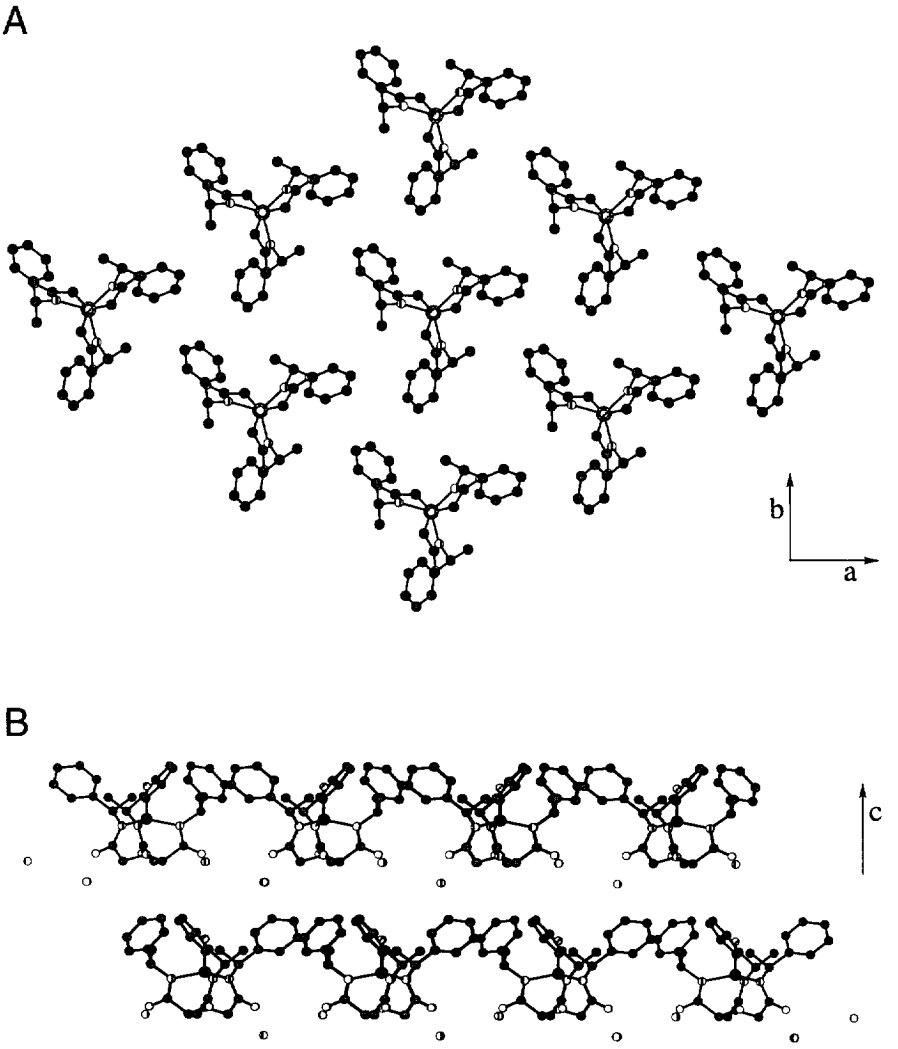


Fig. 6. A portion of the crystal lattice for $[Ni1^{S\text{-}mbz}(F)]^{2-}$ (A) (viewed along the $a, b$ plane) and (B) (viewed along the $b, c$ plane) showing the positions of the nitrogen atoms of the $Et_4N^+$ ions. Hydrogens have been omitted for clarity.

severely disordered and only the positions of the nitrogen atoms could be determined. Nevertheless, two potentially useful structural features can be gleaned from the relative positioning of these anions and cations in the crystal lattice. First, all the Ni–F bonds in the $[Ni1^{S\text{-}mbz}(F)]^{2-}$ anions are oriented in the same direction, coincident with the crystallographic $c$-axis (Figs. 7 and 8). This alignment of Ni–F bonds, which should have large dipoles, may lead this crystalline salt to have a large net dipole moment which is a prerequisite for important physical properties, such as

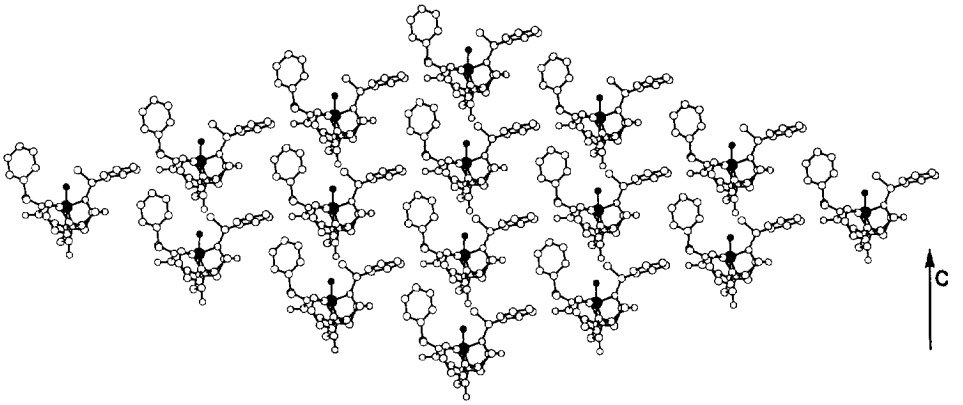


Fig. 7. A portion of the crystal lattice for $[Ni1^{S\text{-}mbz}(F)]^{2-}$ showing the alignment of the Ni–F bonds. Hydrogens have been omitted for clarity.

nonlinear optical activity. Second, as illustrated in Fig. 8, six-fold symmetric chiral channels are dispersed throughout the lattice that are walled by the chiral tripodal arms of the $[Ni1^{S\text{-}mbz}(F)]^{2-}$ anions. The channels in this lattice have diameters of $\sim$11.5 Å and are filled with tetraethylammonium cations. The role of the cations in the channel formation is not presently known because the disorder in the ethyl groups has hindered any detailed structural analysis. The effects of cations on the assembly process are currently being assessed by the use of different cations during crystal growth.

## 4. Summary

In this work, we have shown that by using the self-complementary chiral tripodal ligand $H_31^{S\text{-}mbz}$, new chiral crystals can be synthesized. For $H_31^{S\text{-}mbz}$, $C_3$-symmetric chiral columns can assemble in the crystal phase where each column is stabilized by a combination of hydrogen bonds and aryl–aryl interactions. Intercolumnar assembly is driven by the clustering of edge-to-face aryl and methyl-to-aryl interactions. The effect of placing optically pure (*S*)-(−)-(α)-methylbenzyl groups at the amide ends of the tripods is evident by the alignment of individual molecules in each column and the positioning of the columns within the crystal lattice. A non-centrosymmetric crystal lattice is also obtained by replacing the protons in $H_31^{S\text{-}mbz}$ with an Ni–F moiety to form the chiral salt $[NEt_4]_2[Ni1^{S\text{-}mbz}(F)]$. Although the molecular structures of $H_31^{S\text{-}mbz}$ and $[Ni1^{S\text{-}mbz}(F)]^{2-}$ differ significantly, they both have molecular $C_3$-symmetry. The molecular structure of $[Ni1^{S\text{-}mbz}(F)]^{2-}$ suggests that the orientation of the appended methylbenzyl groups is influenced by the binding of the fluoro ligand, with both the methyl and aryl groups involved in CH···F interactions. Edge-to-face interactions between chiral ligands are the dominant interanion interactions leading to alternating layers of anions and cations within the crystal lattice.

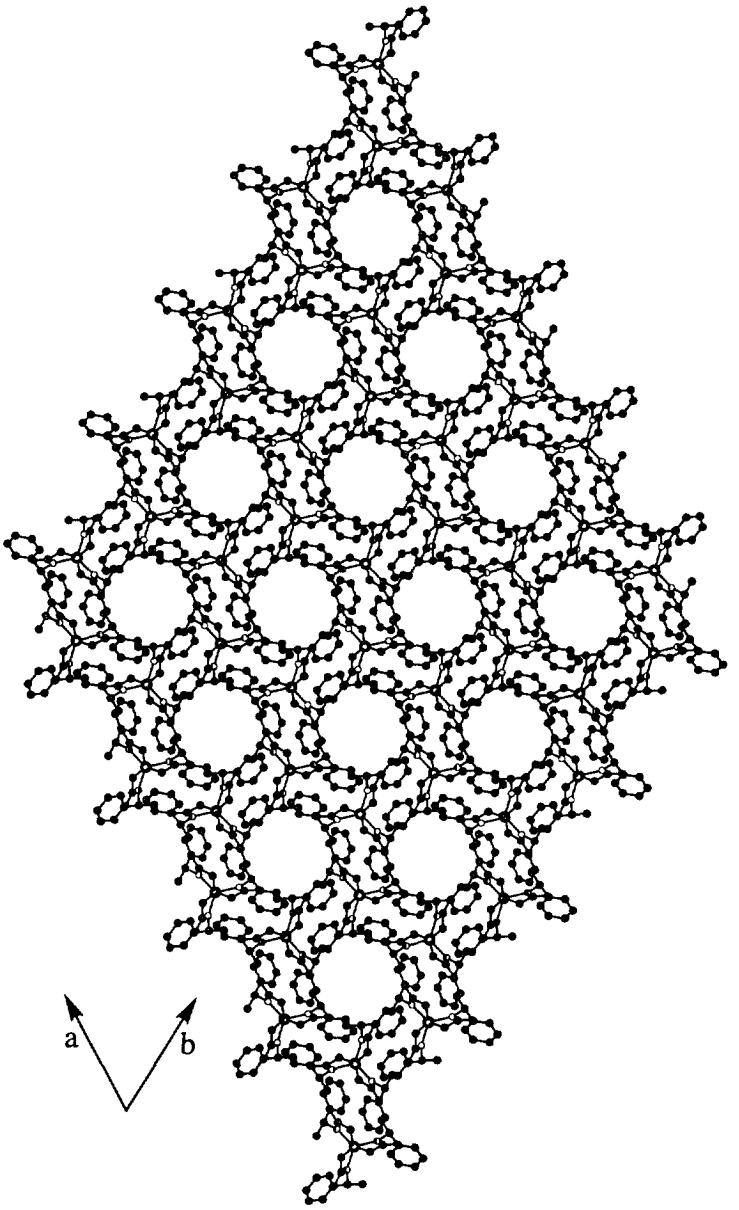


Fig. 8. A portion of the crystal lattice for $[Ni1^{S\text{-}mbz}(F)]^{2-}$ (viewed along the $a$, $b$ plane). The $Et_4N^+$ ions and the hydrogens have been omitted for clarity.

This results in the alignment of the molecular Ni–F bonds and a chiral channel structure: both of these structural properties may be useful in developing new metal-based crystalline materials.

## Acknowledgements

Acknowledgement is made to the NIH (GM50781 to A.S.B.) for the financial support of this research.

## References

[1] J.-M. Lehn, Angew. Chem., Int. Ed. Engl. 29 (1990) 1304.
[2] R. Robson, B.F. Abrahams, S.R. Batten, R.W. Gable, B.F. Hoskins, T. Bein (Eds.), Supramolecular Architecture, American Chemical Society, Washington, DC, 1992, p. 256.
[3] L. Fabbrizzi, A. Poggi (Eds.), Transition Metals in Supramolecular Chemistry, Kluwer Academic, Dordrecht, 1994.
[4] K.A. Hirsch, S.R. Wilson, J.S. Moore, Inorg. Chem. 36 (1997) 2960 and references cited therein
[5] T. Kawamoto, B.S. Hammes, B. Haggerty, G.P.A. Yap, A.L. Rheingold, A.S. Borovik, J. Am. Chem. Soc. 118 (1996) 285.
[6] T. Kawamoto, O. Prakash, R. Ostrander, A.L. Rheingold, A.S. Borovik, Inorg. Chem. 34 (1995) 4294.
[7] B.S. Hammes, D. Ramos-Maldonado, G.P.A. Yap, L. Liable-Sands, A.L. Rheingold, V.G. Young, A.S. Borovik, Inorg. Chem. 36 (1997) 3210.
[8] M. Ray, A.P. Golombek, M.P. Hendrich, V.G. Young, A.S. Borovik, J. Am. Chem. Soc. 118 (1996) 6084.
[9] M. Ray, G.P.A. Yap, A.L. Rheingold, A.S. Borovik, J. Chem. Soc., Chem. Commun. (1995) 1777.
[10] M. Ray, B.S. Hammes, G.P.A. Yap, A.L. Rheingold, A.S. Borovik, in preparation.
[11] R. Wyler, J. de Mendoza, J. Rebek Jr., Angew. Chem., Int. Ed. Engl. 32 (1993) 1699.
[12] B.N. Figgis, R.S. Nyholm, J. Chem. Soc. (1958) 4190.
[13] A.L. Spek, Acta Crystallogr. A46 (1990) C34.
[14] S.K. Burley, G.A. Petsko, J. Am. Chem. Soc. 108 (1986) 7995.
[15] S.K. Burley, G.A. Petsko, Adv. Protein Chem. 39 (1988) 125.
[16] C.A. Hunter, J.K.M. Sanders, J. Am. Chem. Soc. 112 (1990) 5525.
[17] C.A. Hunter, Chem. Soc. Rev. (1994) 101 and references cited therein.
[18] P. Hobza, H.L. Selzle, E.W. Schlag, J. Am. Chem. Soc. 116 (1994) 3500.
[19] S.K. Burley, G.A. Petsko, Science (Washington, DC) 229 (1985) 23.
[20] G.R. Desiraju, A. Gavezzotti, J. Chem. Soc., Chem. Commun. (1989) 621 and references cited therein.
[21] A.V. Muehldorf, D. Van Engen, J.C. Warner, A.D. Hamilton, J. Am. Chem. Soc. 110 (1988) 6561.
[22] C.A. Hunter, J. Chem. Soc., Chem. Commun. (1991) 749.
[23] F. Erkang, J. Yang, S.J. Geib, T.C. Stoner, M.D. Hopkins, A.D. Hamilton, J. Chem. Soc., Chem. Commun. (1995) 1251.
[24] H.C. Freeman, J.M. Guss, R.L. Sinclair, J. Chem. Soc., Chem. Commun. (1968) 485.
[25] R. Machida, E. Kimura, Y. Kushi, Inorg. Chem. 25 (1986) 3461.
[26] E. Kimura, T. Koike, Y. Iitak, Inorg. Chem. 29 (1990) 4621.
[27] J. Emsley, M. Arif, J. Chem. Soc., Dalton Trans. (1989) 1273.
[28] P. Halasyamani, M.J. Willis, C.L. Stern, K.R. Poeppelmeier, Inorg. Chim. Acta 240 (1995) 109.
[29] K. Toriumi, T. Ito, Acta Crystallogr. B37 (1981) 240.
[30] P. Murray-Rust, W.C. Stallings, C.T. Monti, R.K. Preston, J.P. Glusker, J. Am. Chem. Soc. 105 (1983) 3207.
[31] G.D. Desiraju, Crystal Engineering: The Design of Organic Solids, Elsevier, New York, 1989.
[32] G.R. Desiraju, Angew. Chem., Int. Ed. Engl. 34 (1995) 2311.